United States Department of Commerce
Technology Administration
National Institute of Standards and Technology

NIST Technical Note 1355-R

Transmission/Reflection and Short-Circuit Line Methods for Measuring Permittivity and Permeability

James Baker-Jarvis
Michael D. Janezic
John H. Grosvenor, Jr.
Richard G. Geyer

Transmission/Reflection and Short-Circuit Line Methods for Measuring Permittivity and Permeability

James Baker-Jarvis
Michael D. Janezic
John H. Grosvenor, Jr.
Richard G. Geyer

Electromagnetic Fields Division
Electronics and Electrical Engineering Laboratory
National Institute of Standards and Technology
325 Broadway
Boulder, Colorado 80303-3328

December 1993

U.S. DEPARTMENT OF COMMERCE, Ronald H. Brown, Secretary
TECHNOLOGY ADMINISTRATION, Mary L. Good, Under Secretary for Technology
NATIONAL INSTITUTE OF STANDARDS AND TECHNOLOGY, Arati Prabhakar, Director

National Institute of Standards and Technology Technical Note
Natl. Inst. Stand. Technol., Tech. Note 1355-R, 236 pages (December 1993)
CODEN:NTNOEF

U.S. GOVERNMENT PRINTING OFFICE
WASHINGTON: 1993

For sale by the Superintendent of Documents, U.S. Government Printing Office, Washington, DC 20402-9325

Contents

Abstract

The transmission/reflection and short-circuit line methods for measuring complex permittivity and permeability of materials in waveguides and coaxial lines are examined. Equations for complex permittivity and permeability are developed from first principles. In addition, new formulations for the determination of complex permittivity and permeability independent of reference plane position are derived. For the one-sample transmission/reflection method and two-position short-circuit line measurements, the solutions are unstable at frequencies corresponding to integral multiples of one-half wavelength in the sample. For two-sample methods the solutions are unstable for frequencies where both samples resonate simultaneously. Criteria are given for sample lengths to maintain stability. An optimized solution is also presented for the scattering parameters. This solution is stable over all frequencies and is capable of reducing scattering parameter data on materials with higher dielectric constant. An uncertainty analysis for the various techniques is developed and the results are compared. The errors incurred due to the uncertainty in scattering parameters, length measurement, and reference plane position are used as inputs to the uncertainty models.

Key words: Calibration; coaxial line; dielectric constant; loss factor; magnetic materials; microwave measurements; permeameter; permeability measurement; permittivity measurement; reflection method; short-circuit; transmission; uncertainty; waveguide.

Chapter 1

Introduction

The goal of this report is to review and critically evaluate various transmission line measurement algorithms for combined permeability and permittivity determination and to present results and uncertainty analysis for the techniques.

There is continual demand to measure accurately the magnetic and dielectric properties of solid materials. Over the years there has been an abundance of methods developed for measuring permeability and permittivity. Almost all possible perturbations or variations of existing methods have been proposed for measurements. These techniques include free-space methods, open-ended coaxial probe techniques, cavity resonators, full-body resonance techniques, and transmission-line techniques. Each method has its range of applicability and its own inherent limitations. For example, techniques based on cavities are accurate, but not broadband. Nondestructive techniques, although not most accurate, allow the maintenance of material integrity. Transmission line techniques are the simplest of the relatively accurate ways of measuring permeability and permittivity of materials. Transmission line measurements usually are made in waveguide or coaxial lines. Measurements are made in other types of transmission lines for special applications, but for precise measurements, rectangular waveguides and coaxial lines are usually used. The three major problems encountered in transmission line measurements are air gaps, half-wavelength resonances, and overmoding.

Coaxial lines are broadband in the TEM mode and therefore are attractive for permittivity and permeability measurements. The problem with coaxial lines, however, is that due to the discontinuity of the radial electric field, any air gap around the center conductor degrades the measurement by introducing a large measurement uncertainty. Belhadj-Tahar et al. [1] have attempted to circumvent these difficulties with the development of a technique for a plug of material at the end of a coaxial line. In Belhadj-Tahar's approach there is no center conductor hole. However, higher modes are excited at the transition between the plug and the center conductor which complicates the analysis. Due to the complexity

of the method it is not apparent at this time whether this approach will replace the more traditional single-mode models.

Transmission line techniques generally fall into the following categories:

- Off-resonance waveguide and coaxial line, full scattering parameter, 2-port measurements.
- Off-resonance short-circuit line, 1-port measurements.
- Open-circuit techniques.
- Resonant transmission-line techniques.

The topic of this report will be the first two categories. We will also examine direct inductance measurement, which uses permeameter techniques. The off-resonance techniques can be broadly grouped into two categories:

- Point-by-point or uncorrelated-point techniques.
- Multi-point or correlated-point techniques.

The point-by-point technique is at present the most widely used reduction technique and consists of solving the relevant scattering equations at single points. Multi-point techniques consist of solving the nonlinear scattering equations using nonlinear least square algorithms.

Due to their relative simplicity, the off-resonance waveguide and coaxial line transmission/reflection (TR) and short-circuit line (SCL) methods are presently widely used broadband measurement techniques. In these methods a precisely machined sample is placed in a section of waveguide or coaxial line and the scattering parameters are measured, preferably by an automatic network analyzer (ANA). The relevant scattering equations relate the measured scattering parameters to the permittivity and permeability of the material. One limitation of these techniques is that they require cutting of the sample and therefore these techniques do not fall under the general category of nondestructive testing methods. Another limitation is that these techniques require a small sample and therefore the resonance characteristics of large sheets of the material are not studied. Network analyzers have improved over the last years to a point where broad frequency coverage and accurate measurement of scattering parameters are possible. This broadband capability unearths another limitation of present algorithms, that is, the instability of the measurement in the vicinity of resonant frequencies.

In this report we assume that the materials under test are isotropic, homogeneous, and in a demagnetized state. The solutions obtained in this report are both single-frequency techniques and multiple frequency techniques. For the TR measurement, the system of equations contains as variables the complex permittivity and permeability, the two reference

plane positions, and, in some applications, the sample length. In the T/R procedure we have more data at our disposal than in SCL measurements, since we have all four of the scattering parameters. In SCL measurements the variables are complex permittivity and permeability, sample length, distance from sample to short-circuit termination, and reference plane positions. However, in most problems we know the sample length, reference plane position, and distance from the reflector to the sample. In these cases we have four unknown quantities (complex permittivity and permeability) and therefore require four independent real equations to solve for these variables. These equations can be generated by taking reflection coefficient data at two positions in the transmission line, thus yielding the equivalent of four real equations for the four unknown quantities. A problem encountered in measurements is the transformation of S-parameter measurements at the calibration reference planes to the air-sample interface. This transformation requires knowledge of the position of the sample in the sample holder. Information on reference plane position is limited in many applications. The port extension and gating features of network analyzers are of some help in determining reference plane position, but do not completely solve the problem. Equations that are independent of reference plane position are desirable.

Most of the present transmission-line techniques [2,3,4], with some variations, are based on the procedure developed by Nicolson and Ross [5] and Weir [6] for obtaining 2-port, off-resonance, broadband measurements of permeability and permittivity. In the Nicolson-Ross-Weir (NRW) procedure the equations for the scattering parameters are combined in such a fashion that the system of equations can be decoupled. This procedure yields an explicit expression for the permittivity and permeability as a function of the S-parameters. These equations are not well-behaved for low-loss materials at frequencies corresponding to integral multiples of one-half wavelength in the sample. In fact, the NRW equations are divergent, due to large phase uncertainties for very low-loss materials at integral multiples of one-half wavelength in the material. Many researchers avoid this problem by measuring samples which are less than one-half wavelength long at the highest measurement frequency. The advantage of the NRW approach is that it yields both permittivity and permeability over a large frequency band. As a special case of the NRW equations, Stuchly and Matuszewski [7] found solutions to the scattering equations for nonmagnetic materials and derived two explicit equations for the permittivity. Delecki and Stuchly [8] have studied the uncertainty analysis for infinitely long samples using the bilinear and Schwarz-Christoffel transformations. Franceschetti [9] was one of the first to perform a detailed uncertainty analysis for TR measurements. Ligthart [10] developed an analytical method for permittivity measurements at microwave frequencies using an averaging procedure. In Ligthardt's study, a single-moded cylindrical waveguide was filled with a homogeneous dielectric with a moving short-circuit termination positioned beyond the sample. This study focused primarily on single-frequency measurements rather than on broadband measurements.

The short-circuit line (SCL) method was introduced by Roberts and von Hippel [11] over fifty years ago as an accurate broadband measurement procedure. The SCL measure-

ment method uses data obtained from a short-circuit 1-port measurement to calculate the dielectric and magnetic properties. SCL is useful when 2-port measurements are not possible, for example, in high temperature measurements [12] and remote sensing applications. When an ANA is used, the sample is positioned in either a waveguide or coaxial line and the reflection coefficient is measured. The determination of the permittivity and permeability usually proceeds by solving a transcendental equation that involves the sample length, sample position, and reflection coefficient. With modern computer systems, iterative solutions of the resulting transcendental equations are easy to implement. However, they require an initial guess. The resultant nonlinear equations have an infinite number of solutions due to periodic functions. The physical solution can be determined by group delay arguments or by measuring two samples with differing lengths. Much of the theory developed for the SCL technique was developed for use with a slotted line. Present-day network analyzers usually measure scattering parameters. Therefore in this report we derive equations from a scattering approach.

The SCL method has endured over the years, and as a result there is an extensive literature. In this report we attempt to review only the most relevant work on the subject. Short-circuit line methods can be broadly separated into *two- position techniques* and *two-sample techniques*. In the *two-position technique* 1-port scattering parameters are measured for a sample in two different positions in the sample holder. In the *two-sample technique* two samples of different lengths are machined from the same material and scattering parameters are measured with each sample pressed against the short-circuit termination. Szendrenyi [13] developed an algorithm for the case in which the length of one sample is precisely twice the length of the other sample. In this special case, they found an explicit solution.

Mattar and Brodwin [14] have described a variable reactance termination technique for permittivity determination. Maze [15] has presented an optimized-solution technique where at each frequency scattering parameters are taken for various short-circuit termination positions. Dakin and Work [16] developed a procedure for low-loss materials and Bowie and Kelleher [17] presented a rapid graphical technique for solving the scattering equations. Other authors have presented methods using measurements on two or more sample lengths [18]. Most of the literature to date has focused on permittivity determination. In the few works that have addressed the combined permeability and permittivity problem, many details have been left unresolved.

Recently Chao [19] presented SCL measurements results with a slotted line and also an uncertainty analysis for single frequency measurements. Chao found that accuracy was reduced when the reflection coefficient is dominated by the front face contribution.

The SCL measurement may use either a fixed or movable short-circuit device. The advantage of a moving short-circuit termination [2] is the possibility for making many separate measurements at a given frequency with the sample placed in either a high electric or magnetic field region [15]. Generally, a maximum in electric field strength is advantageous for permittivity measurements, whereas a maximum in magnetic field strength is

advantageous for permeability measurements.

When only permittivity is required, a single measurement at a given frequency suffices, whereas when both permeability and permittivity are to be determined, it is necessary to carry out two independent measurements at each frequency. There are various contributions to the uncertainties in the SCL method. These uncertainties include network analyzer uncertainties, sample gaps, wall and reflection losses, and measurement of sample dimensions. There are also uncertainties in the location of the sample reference planes and in the distance from sample to the short-circuit termination. The uncertainty in the network analyzer parameters are sometimes documented by the manufacturer [3].

In this report we develop relevant equations from first principles. These equations apply to ANA systems. We will examine the various approaches for combined determination of permeability and permittivity, and study the uncertainty in the measurement process. The special case of repeated measurements on a sample of fixed length is treated in detail.

Chapter 2

Theory for Coaxial Line and Rectangular Waveguide Measurements of Permittivity and Permeability

2.1 Theory

The goal of this chapter is to present various approaches for obtaining both the permeability and permittivity from transmission line scattering data. In the TR measurement, a sample is inserted into either a waveguide or a coaxial line, and the sample is subjected to an incident electromagnetic field [see figure 2.1]. The scattering equations are found from an analysis of the electric field at the sample interfaces. In order to determine the material properties from scattering data, it is necessary to understand the structure of the electromagnetic field in waveguides. In developing the scattering equations usually only the fundamental waveguide mode is assumed to exist. In this report we develop the theory for multimode solutions. However, the numerical algorithms presented will be valid only for the fundamental mode.

2.1.1 Decomposition into TE, TM, and TEM Modes

In this section we briefly review the theory of modes in transmission lines. It is possible to decompose the fields in a waveguide at a given frequency into the complete set of TE, TM,

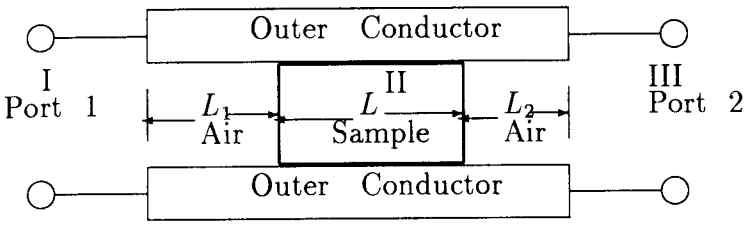

Figure 2.1: A dielectric sample in a transmission line and the incident and reflected electric field distributions in the regions I, II, and III. Port 1 and port 2 denote calibration reference plane positions.

and TEM modes. In our model at hand we assume:

- There is a propagation direction in the guide which we call $\vec{z}$.
- The cross-sectional area of the guide is perpendicular to $\vec{z}$ and constant throughout the length of the guide.

Electromagnetic fields in a sourceless region satisfy

$$\nabla \times \nabla \times \vec{E} = -j\omega\nabla\mu \times \vec{H} + k^2\vec{E} \ , \tag{2.1}$$

$$\nabla \times \nabla \times \vec{H} = j\omega\nabla\epsilon \times \vec{E} + k^2\vec{H} \ , \tag{2.2}$$

where $k = -j\gamma$ is the wave number.

In this report we assume that there are no sources of electric and magnetic fields in the guide ($\vec{J} = 0$) and there no free charge build up ($\nabla \cdot \vec{D} = 0$). Further we assume that the material parameters are not spatially dependent. However, step function discontinuities are assumed to exist between the sample and air gap. The step function discontinuities in the equations can contribute a delta function term in derivatives. With these assumptions, the fields satisfy homogeneous Helmholtz equations,

$$\nabla^2\vec{E} + k^2\vec{E} = 0 \ , \tag{2.3}$$

$$\nabla^2\vec{H} + k^2\vec{H} = 0 \ . \tag{2.4}$$

The time-dependent fields can be expanded in terms of modes

$$\vec{\mathcal{E}}(\vec{r},t) = \frac{1}{2\pi}\int_{-\infty}^{\infty} d\omega \sum_n \vec{E}_n(\vec{r}_T,\omega)\exp(\pm\gamma_n z)\exp(j\omega t) \ , \tag{2.5}$$

$$\vec{\mathcal{H}}(\vec{r},t) = \frac{1}{2\pi}\int_{-\infty}^{\infty} d\omega \sum_n \vec{H}_n(\vec{r}_T,\omega)\exp(\pm\gamma_n z)\exp(j\omega t)\ , \tag{2.6}$$

where $\vec{r}_T$ is a transverse vector, E_n, H_n are the amplitudes of the modes, and

$$\gamma_n = j\sqrt{\frac{\omega^2\mu_R^*\epsilon_R^*}{c_{vac}^2} - \left(\frac{2\pi}{\lambda_{nc}}\right)^2}\ , \tag{2.7}$$

$$\gamma_o = j\sqrt{\left(\frac{\omega}{c_{lab}}\right)^2 - \left(\frac{2\pi}{\lambda_{nc}}\right)^2}\ , \tag{2.8}$$

where γ_o, γ_n are the propagation constants in vacuum and material, respectively. Also $j = \sqrt{-1}$, c_{vac} and c_{lab} are the speed of light in vacuum and laboratory, ω is the angular frequency, λ_{nc} is the cutoff wavelength of the nth mode, ϵ_o and μ_o are the permittivity and permeability of vacuum, ϵ_R^* and μ_R^* are the complex permittivity and permeability relative to a vacuum.

Since these modes satisfy a Sturm-Liouville problem, we know that the totality of these waves forms a complete set of functions, and therefore an eigenfunction expansion property exists for this system. The Laplacian separates in the coordinate systems used in this report, and therefore the fields can be separated into transverse (T) and longitudinal (z) components:

$$\vec{E} = \vec{E}_T + E_z\vec{z}\ , \tag{2.9}$$

$$\vec{H} = \vec{H}_T + H_z\vec{z}\ . \tag{2.10}$$

The component E_z is the generator of the TM mode (see Appendix) and the H_z component is the generator of the TE mode. Since the TE, TM, and TEM modes form a complete set of functions, we can expand the transverse Fourier-transformed fields as

$$\begin{aligned}\vec{E}_T(\vec{r},\omega) = &\\ &\sum_{n=1}^{\infty}\{E_{nTE}^+\exp(-\gamma_n z) + E_{nTE}^-\exp(\gamma_n z)\}\vec{E}_{T(TE)}(\vec{r}_T)\\ &+\sum_{n=1}^{\infty}\{E_{nTM}^+\exp(-\gamma_n z) + E_{nTM}^-\exp(\gamma_n z)\}\vec{E}_{T(TM)}(\vec{r}_T)\\ &+\sum_{n=1}^{N-1}\{E_{nTEM}^+\exp(-\gamma_n z) + E_{nTEM}^-\exp(\gamma_n z)\}\vec{E}_{T(TEM)}(\vec{r}_T)\ ,\end{aligned} \tag{2.11}$$

$$\vec{H}_T(\vec{r},\omega) =$$

$$\sum_{n=1}^{\infty} \frac{1}{Z_{nTE}} \{E_{nTE}^{+} \exp(-\gamma_n z) - E_{nTE}^{-} \exp(\gamma_n z)\}(\vec{z} \times \vec{E}_{T(TE)})(\vec{r}_T))$$
$$+ \sum_{n=1}^{\infty} \frac{1}{Z_{nTM}} \{E_{nTM}^{+} \exp(-\gamma_n z) - E_{nTM}^{-} \exp(\gamma_n z)\}(\vec{z} \times \vec{E}_{T(TM)}(\vec{r}_T))$$
$$+ \sum_{n=1}^{N-1} \sqrt{\frac{\epsilon}{\mu}} \{E_{nTEM}^{+} \exp(-\gamma_n z) - E_{nTEM}^{-} \exp(\gamma_n z)\}(\vec{z} \times \vec{E}_{T(TEM)}(\vec{r}_T)) \quad (2.12)$$

where N is the number of disjoint conductors and $(\pm)$ denotes forward and backward traveling waves. The coefficients E_n depend on the transverse components, and the wave impedances are

$$Z_{TM} = \frac{\gamma_n}{j\omega\epsilon} , \quad (2.13)$$

$$Z_{TE} = \frac{j\omega\mu}{\gamma_n} . \quad (2.14)$$

Although the sums for the TE and the TM waves in eqs (3.11) and (2.12) approach ∞, in many problems of practical interest, some of the coefficients in the sums vanish. Two or more modes may have the same eigenvalue; the eigenvectors in these cases are called *degenerate*.

In order to solve eq (2.3) it is expeditious to break up the Laplacian into transverse and longitudinal components,

$$\nabla^2 \vec{E} = \nabla_T^2 \vec{E} + \frac{\nabla^2 \vec{E}}{\partial z^2} , \quad (2.15)$$

where

$$\frac{\partial^2 \vec{E}}{\partial z^2} = \gamma^2 \vec{E} , \quad (2.16)$$

and the transverse Laplacian satisfies by eq (2.3)

$$\nabla_T^2 \vec{E} = -(k^2 + \gamma^2)\vec{E} \equiv -k_c^2 \vec{E} , \quad (2.17)$$

where k_c is the cutoff wavenumber. If ϵ has a dependence on transverse coordinates in terms of a step discontinuity, then γ also has a transverse dependence. In Appendix A, the details of the derivations of the fields are reviewed.

2.1.2 Imperfect Sample Geometry

In the case of perfect or near perfect samples and sample holders, γ is independent of the transverse coordinates and therefore different eigenfunctions for the transverse components

in the air and sample regions possess an orthogonality condition [see Appendix A]. In such cases it is possible to match mode by mode, and the coefficients are decoupled. However, when samples and sample holder are not perfectly formed or are slightly inhomogeneous, both μ and ϵ have a weak dependence on the transverse coordinates of the guide and therefore the different transverse eigenfunctions in the sample are not orthogonal to the transverse eigenfunctions in the air section. The modes of imperfect samples cannot be separated and matched mode by mode. The imperfections in the sample generate evanescent waves at the sample-material interface. These modes may propagate in the sample, but they decay exponentially outside of the sample.

For an imperfect sample, the fields in the regions I, II, and III are found from an analysis of the electric field at the sample interfaces. We assume that the incident electric field is the TE_{10} mode in rectangular waveguide and TEM in coaxial line. As the wave propagates from the air-filled region into the sample, some of the energy carried in the wave will convert into higher order modes. However, it is necessary to consider only the transverse components of the fields when matching boundary conditions. In the following we assume that gaps or other imperfections can exist in and around the sample. We further assume that the imperfections are such that the Laplacian can be separated into transverse and longitudinal components. If the imperfections are azimuthally symmetric, then only the H_ϕ magnetic field component is assumed to exist. If we assume the vector component of the normalized electric fields E_I, E_{II}, and, E_{III}[1] in the regions I, II, and III, we can write for N modes

$$E_I = \underbrace{\exp(-\gamma_{o1}z)}_{\text{incident wave}} + S_{11}\exp(\gamma_{o1}z) + \sum_{i=2}^{N} \underbrace{C_i(\vec{z}_T)\exp(\gamma_{oi}z)}_{\text{evanescent}}\Big] , \tag{2.18}$$

$$E_{II} = \sum_{i=1}^{N}[D_i(\vec{z}_T)\exp(-\gamma_{mi}z) + E_i(\vec{z}_T)\exp(\gamma_{mi}z)] , \tag{2.19}$$

$$E_{III} = S_{21}\underbrace{\exp(-\gamma_{o1}(z-L))}_{\text{transmitted wave}} + \sum_{i=2}^{N} \underbrace{[F_i(\vec{z}_T)\exp(-\gamma_{oi}(z-L))]}_{\text{evanescent}} , \tag{2.20}$$

where C_i, D_i, E_i, F_i are the modal coefficients, which may depend on the transverse coordinates. Also γ_{oi}, γ_{mi} are the propagation constants of the ith mode in vacuum and material respectively. We assume that we are operating the waveguide at such a frequency that only the fundamental mode is a propagating mode in the air section of the guide. The other modes are evanescent in the air section of the guide, but may be propagating in the material-filled section. There may be additional modes produced by mode conversion for

[1]TEM mode in a coaxial line or the TE_{10} mode in a waveguide (with a time dependence of $\exp(j\omega t)$ suppressed)

the other components of the electric field, but these are not necessary for specification of the boundary conditions.

In general, the amplitudes in eqs (2.18) to (2.20) are functions of the transverse coordinates. To find the coefficients, it is necessary to match tangential electric and magnetic fields at the interfaces and integrate over the cross- sectional area. Since different transverse eigenfunctions in the air are not orthogonal to transverse eigenfunctions in the sample we cannot separate a particular mode in the sample and match it to the analogous mode in the air. The tangential electric field matching yields

$$\delta_{k1} + (1 - \delta_{k1})c_k = \sum_{j=1}^{N} [A_{kj}d_j + A_{kj}e_j] \ , \tag{2.21}$$

$$[d_k \exp(-\gamma_{mk}L) + e_k \exp(\gamma_{mk}L) = \sum_{j=1}^{N} A_{jk}f_j \ , \tag{2.22}$$

where δ_{ij} is the Kronecker delta and c, e, and f are the integrated coefficients, N is the number of modes, and A_{kj} is the matrix of the coefficients of the integrated transverse eigenfunctions. The transverse component of the magnetic field can be obtained from Maxwell's equations using eqs (2.21) and (2.22). If we match the tangential magnetic field components and integrate over the transverse variables we have

$$[-\frac{\gamma_{01}}{\mu_0}\delta_{k1} + \frac{\gamma_{0k}}{\mu_0}(1 - \delta_{k1})c_k] = \sum_{j=1}^{N} \frac{\gamma_{mj}}{\mu}[-A_{kj}d_j + A_{kj}e_j] \ , \tag{2.23}$$

$$[-d_k\frac{\gamma_{mk}}{\mu} \exp(-\gamma_{mk}L) + \frac{\gamma_{mk}}{\mu}e_k \exp(\gamma_{mk}L) = -\sum_{j=1}^{N} A_{jk}f_j\frac{\gamma_{0j}}{\mu_0} \ , \tag{2.24}$$

where L is the sample length and

$$L_{air} = L + L_1 + L_2 \ . \tag{2.25}$$

These boundary conditions yield a linear system of equations for the coefficients. Various cutoff frequencies and operating frequencies are given in tables 2.1 and 2.2.

The difficulties in solving the full mode problem in eqs (2.21) to (2.24) is that the coefficients of the matrix A_{kj} are not generally known precisely unless the complete boundary value problem is solved for each sample. These coefficients are known only for simple, well-defined geometries and not for samples with unknown air gaps or complicated inhomogeneities.

Table 2.1: Cutoff frequencies for TE_{10} mode in rectangular waveguide.

EIA WR	Band	Cutoff frequency(GHz)
650	L	0.908
430	W	1.372
284	S	2.078
187	C	3.152
90	X	6.557
42	K	14.047
22	Q	26.342

Table 2.2: Rectangular waveguide dimensions and operating frequencies in air.

EIA WR	Band	a (cm)	b (cm)	TE_{10} Operating frequency(GHz)
650	L	16.510	8.255	1.12 - 1.70
430	W	10.922	5.461	1.70 - 2.60
284	S	7.710	3.403	2.60 - 3.95
187	C	4.754	2.214	3.95 - 5.85
90	X	2.286	1.016	8.20 - 12.40
42	K	1.067	0.432	18.0 - 26.5
22	Q	0.569	0.284	33.0 - 50.0

2.1.3 Perfect Sample in Waveguide

As a special case of the formalism developed in the previous section we consider a perfect sample in a perfect waveguide as indicated in figure 2.1. In this case no mode conversion occurs because the eigenfunctions in the air and sample regions are orthogonal with respect to cross-sectional coordinates. Therefore the modes may be decoupled and the evanescent modes are not of concern. This is a special case of eqs (2.21) to (2.25). In this case we need to be concerned only with the fundamental mode in the guide. The electric fields in the sample region $z \in (0, L)$ for a coaxial line with a matched load and with the radial dependence written explicitly are

$$E_I = \frac{1}{r}[\exp(-\gamma_o z) + S_{11}\exp(\gamma_o z)] \ . \tag{2.26}$$

$$E_{II} = \frac{1}{r}(C_2[\exp(-\gamma_1 z) + C_3\exp(\gamma_1 z)] \ . \tag{2.27}$$

$$E_{III} = \frac{1}{r}[S_{21}\exp(-\gamma_o(z-L))] \ . \tag{2.28}$$

When these equations are integrated over the cross-sectional surface area, the radial dependence is the same for each region of the waveguide.

The constants in the field equations are again determined from the boundary conditions. The boundary condition on the electric field is the continuity of the tangential component at the interfaces. The tangential component can be calculated from Maxwell's equations given an electric field with only a radial component. The higher modes in eqs (2.18) to (2.20) are evanescent in the air-filled section of the guide. TM modes can be treated similarly. The details of the boundary matching for the TE_{10} case are described in a previous report on dielectric materials [26,27]. The boundary condition for the magnetic field requires the additional assumption that no surface currents are generated. If this condition holds, then the tangential component of the magnetic field is continuous across the interface. The tangential component can be calculated from Maxwell's equations for an electric field with only a radial component. For a 2-port device the expressions for the measured scattering parameters are obtained by solving eqs (2.18) through (2.20) subject to the boundary conditions. We assume that $S_{12} = S_{21}$. The explicit expressions for a sample in a waveguide a distance L_1 from the port-1 reference plane to the sample front face and L_2 from the sample back face to the port-2 calibration plane are related. The S-parameters measured by the device reference planes are related to the S-parameters at the sample face S' by [26]

$$\overline{\overline{S}}' = \overline{\overline{\Phi}}\,\overline{\overline{S}}\,\overline{\overline{\Phi}} \ , \tag{2.29}$$

where

$$\bar{\bar{\Phi}} = \begin{pmatrix} \exp(j\phi_1) & 0 \\ 0 & \exp(j\phi_2) \end{pmatrix} , \tag{2.30}$$

and $\phi_1 = j\gamma_0 L_1$ and $\phi_2 = j\gamma_0 L_2$. The S-parameters are defined in terms of the reflection coefficient Γ and transmission coefficient z by:

$$S_{11} = R_1^2 \left[\frac{\Gamma(1-z^2)}{1-\Gamma^2 z^2} \right] , \tag{2.31}$$

$$S_{22} = R_2^2 \left[\frac{\Gamma(1-z^2)}{1-\Gamma^2 z^2} \right] , \tag{2.32}$$

$$S_{21} = R_1 R_2 \left[\frac{z(1-\Gamma^2)}{1-\Gamma^2 z^2} \right] , \tag{2.33}$$

where

$$R_1 = \exp(-\gamma_o L_1) , \tag{2.34}$$

$$R_2 = \exp(-\gamma_o L_2) , \tag{2.35}$$

are the respective reference plane transformations. Equations (2.31) through (2.33) are not new and are derived in detail elsewhere [5,28]. We also have an expression for the transmission coefficient Z:

$$Z = \exp(-\gamma L) . \tag{2.36}$$

We define a reflection coefficient by

$$\Gamma = \frac{\frac{\mu}{\gamma} - \frac{\mu_0}{\gamma_0}}{\frac{\mu}{\gamma} + \frac{\mu_0}{\gamma_0}} . \tag{2.37}$$

For coaxial line the cutoff frequency approaches 0, ($\omega_c \to 0$) and therefore Γ reduces to

$$\Gamma = \frac{\frac{c_{vac}}{c_{lab}} \sqrt{\frac{\mu_R^*}{\epsilon_R^*}} - 1}{\frac{c_{vac}}{c_{lab}} \sqrt{\frac{\mu_R^*}{\epsilon_R^*}} + 1} . \tag{2.38}$$

Additionally, S_{21} for the empty sample holder is

$$S_{21}^0 = R_1 R_2 \exp(-\gamma_0 L_a) . \tag{2.39}$$

For nonmagnetic materials, eqs (2.31), (2.32), (2.33) contain ϵ'_R, ϵ''_R, L, and L_a, and the reference plane transformations R_1, R_2 as unknown quantities. Since the equations for S_{12} and S_{21} are theoretically equivalent for isotropic non-gyromagnetic materials, we have four complex equations, eqs (2.31), (2.32), (2.33), (2.39), plus the equation for the length of the air line (2.25), or equivalently, nine real equations for the six unknowns. However, in many applications we know the sample length to high accuracy. For magnetic materials we have eight unknowns. However, we have frequency data for each measurement. Since the lengths are independent of frequency we have an over-determined system of equations. This abundance of information will be exploited in the next chapter.

2.2 Permeability and Permittivity Calculation

2.2.1 Nicolson-Ross-Weir Solutions (NRW)

Nicolson and Ross [5], and Weir [6] combined the equations for S_{11} and S_{21} and discovered a formula for the permittivity and permeability. Their procedure works well at off-resonance where the sample length is not a multiple of one-half wavelength in the material. Near resonance, however, the solution completely breaks down. In the NRW algorithm the reflection coefficient

$$\Gamma_1 = X \pm \sqrt{X^2 - 1} \tag{2.40}$$

is given explicitly in terms of the scattering parameters where

$$X = \frac{1 - V_1 V_2}{V_1 - V_2} , \tag{2.41}$$

and

$$V_1 = S_{21} + S_{11} , \tag{2.42}$$

$$V_2 = S_{21} - S_{11} . \tag{2.43}$$

Note that in the Nicolson-Ross solution the S-parameters must be rotated to the plane of the sample faces in order for the correct group delay to be calculated. The correct root is chosen in eq (2.40) by requiring $|\Gamma_1| \leq 1$. The transmission coefficient Z_1 for the NRW procedure is given by

$$Z_1 = \frac{S_{11} + S_{21} - \Gamma_1}{1 - (S_{11} + S_{21})\Gamma_1} . \tag{2.44}$$

If we define

$$\frac{1}{\Lambda^2} = -[\frac{1}{2\pi L}\ln(\frac{1}{Z_1})]^2 \ , \tag{2.45}$$

then we can solve for the permeability

$$\mu_R^* = \frac{1+\Gamma_1}{(1-\Gamma_1)\Lambda\sqrt{\frac{1}{\lambda_0^2}-\frac{1}{\lambda_c^2}}} \ , \tag{2.46}$$

where λ_0 is the free space wavelength and λ_c is the cutoff wavelength. The permittivity is given by

$$\epsilon_R^* = \frac{\lambda_0^2}{\mu_R^*}[\frac{1}{\lambda_c^2} - [\frac{1}{2\pi L}\ln(\frac{1}{Z_1})]^2] \ . \tag{2.47}$$

Equation (2.45) has an infinite number of roots for magnetic materials, since the logarithm of a complex number is multi-valued. In order to pick out the correct root it is necessary to compare the measured group delay to the calculated group delay. The calculated group delay is related to the change of the wave number k with respect to the angular frequency

$$\tau_{calc.group} =$$

$$-L\frac{d}{df}\sqrt{\frac{\epsilon_R^*\mu_R^* f^2}{c^2} - \frac{1}{\lambda_c^2}} \tag{2.48}$$

$$= -\frac{1}{c^2}\frac{f\epsilon_R^*\mu_R^* + f^2\frac{1}{2}\frac{d(\epsilon_R^*\mu_R^*)}{df}}{\sqrt{\frac{\epsilon_R^*\mu_R^* f^2}{c^2} - \frac{1}{\lambda_c^2}}}L \ . \tag{2.49}$$

The measured group delay is

$$\tau_{meas.group} = \frac{1}{2\pi}\frac{d\phi}{df} \ , \tag{2.50}$$

where ϕ is the phase of Z_1. To determine the correct root, the calculated group delays are found from eq (2.49) for various values of n in the logarithm term in eq (2.45), where $\ln Z = \ln|Z| + j(\theta + 2\pi n)$, where $n = 0, \pm 1, \pm 2, ...$ The calculated and measured group delays are compared to yield the correct value of n. Many researchers think of the NRW solution as an explicit solution; however, due to the phase ambiguity, it is not in the strict sense. Where there is no loss in the sample under test, the NRW solution is divergent at integral multiples of one-half wavelength in the sample. This occurs because the phase of S_{11} cannot be accurately measured for small $|S_{11}|$. Also in this limit both of the scattering equations reduce to the relation $Z^2 \rightarrow 1$, which is only a relation for the phase velocity and

therefore solutions for ϵ_R^* and μ_R^* are not separable. This singular behavior can be minimized in cases where permeability is known *a priori*, as shown in previous work performed by Baker-Jarvis [26].

For magnetic materials there are other methods for solution of the S-parameter equations. In the next section we will describe various solution procedures.

2.2.2 2-Port Solution Where Position is Determined Solely by $L_{airline}$ and L

In order to obtain both the permittivity and the permeability from the S-parameter relations, it is necessary to have at least two independent measurements. These independent measurements could be two samples of different lengths, it could be a full 2-port measurement, or it could be a 1-port SCL measurement of the sample in two different positions in the line. In the full S-parameter solution we solve equations that are invariant to reference planes for ϵ and μ. A set of equations for single-sample magnetic measurements is

$$S_{11}S_{22} - S_{21}S_{12} = \exp\{-2\gamma_0(L_{air} - L)\}\frac{\Gamma^2 - Z^2}{1 - \Gamma^2 Z^2} , \tag{2.51}$$

$$(S_{21} + S_{12})/2 = \exp\{-\gamma_0(L_{air} - L)\}\frac{Z(1 - \Gamma^2)}{1 - \Gamma^2 Z^2} . \tag{2.52}$$

Equation (2.51) is the determinant of the scattering matrix.

Iterative Solution

Equations (2.51) and (2.52) can be solved iteratively or by a technique similar to the NRW technique. In an iterative approach, Newton's numerical method for root determination works quite well. To solve the system it is best to separate the system into four real equations. The iterative solution works well if good initial guesses are available.

Explicit Solution

It is also possible to obtain an explicit solution to eqs (2.51) and (2.52). Let $x = (S_{21}S_{12} - S_{11}S_{22})\exp\{2\gamma_0(L_{air} - L)\}$ and $y = \{(S_{21} + S_{12})/2\}\exp\{\gamma_0(L_{air} - L)\}$, then it can be shown that the physical roots for the transmission coefficient are

$$Z = \frac{x + 1}{2y} \pm \sqrt{\left(\frac{x + 1}{2y}\right)^2 - 1} . \tag{2.53}$$

The reflection coefficient is

$$\Gamma_2 = \pm\sqrt{\frac{x - Z^2}{xZ^2 - 1}} \ . \tag{2.54}$$

The ambiguity in the plus-or-minus sign in eq (2.54) can be resolved by considering the reflection coefficient calculated from S_{11} alone

$$\Gamma_3 = \frac{\alpha(Z^2 - 1) \pm \sqrt{\alpha^2 Z^4 + 2Z^2(2S_{11} - \alpha^2) + \alpha^2}}{2S_{11}Z^2} \ , \tag{2.55}$$

where $\alpha = \exp(-2\gamma_0 L_1)$. The correct root for Γ_3 is picked by requiring $|\Gamma_3| \leq 1$. Note that an estimate of L_1 is needed in eq (2.55). If Γ_2 is compared with Γ_3 then the plus-or-minus sign ambiguity in eq (2.54) can be resolved and therefore Γ_2 is determined. The permeability and permittivity are then

$$\mu_R^* = -\frac{1 + \Gamma_2}{1 - \Gamma_2}\frac{1}{\gamma_0 L}(\ln Z + 2\pi jn) \ , \tag{2.56}$$

$$\epsilon_R^* = \frac{c^2}{\omega^2}[(\frac{2\pi}{\lambda_c})^2 - \frac{1}{L^2}(\ln Z + 2\pi jn)^2]/\mu_R^* \ . \tag{2.57}$$

The correct value of n is picked using the group delay comparison as described in the Nicolson-Ross-Weir technique. At low frequencies the correct roots are more easily identified since they are more widely spaced.

2.2.3 Two Samples of Different Length

Solutions for the material parameters exist when scattering parameters on two samples of differing lengths are measured. Let us consider two samples, one of length L and one of length $\alpha_1 L$ as indicated in figure 2.2.

For independent measurements on two samples where $|S_{21}| > -50dB$ over the frequency band of interest we use only S_{21} measurements. The measurements obtained on the two samples are designated as $S_{21(1)}$ and $S_{21(2)}$ for first and second measurements:

$$S_{21(1)} = \exp\{-\gamma_0(L_{air} - L)\}\frac{Z(1 - \Gamma^2)}{1 - Z^2\Gamma^2} \ , \tag{2.58}$$

$$S_{21(2)} = \exp\{-\gamma_0(L_{air} - \alpha_1 L)\}\frac{Z^{\alpha_1}(1 - \Gamma^2)}{1 - Z^{2\alpha_1}\Gamma^2} \ , \tag{2.59}$$

where

$$Z = \exp(-\gamma L) \ , \tag{2.60}$$

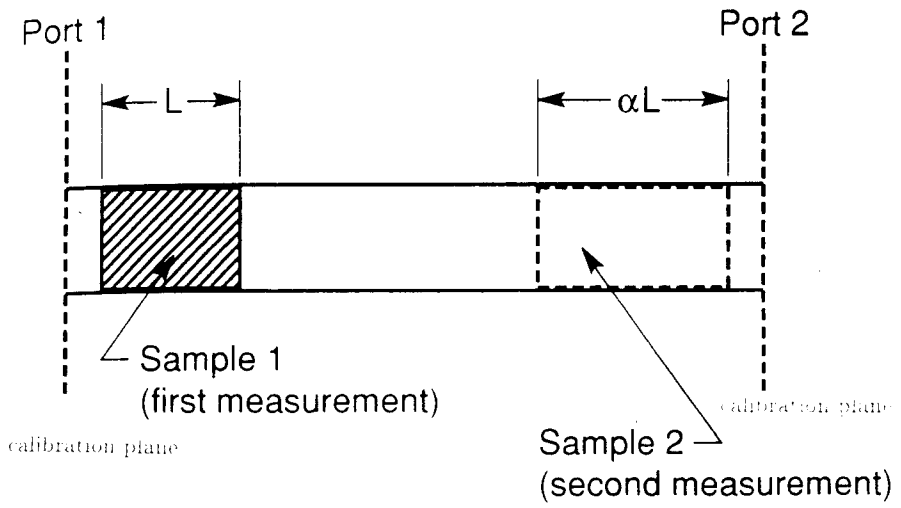

Figure 2.2: A dielectric sample in a transmission line for two sample magnetic measurements

and

$$Z^{\alpha_1} = \exp(-\alpha_1 \gamma L) \ . \tag{2.61}$$

The reflection coefficient is given by eq (2.37). Equations (2.58) and (2.59) can be solved iteratively for ϵ_R^* and μ_R^*.

This solution is unstable for low-loss materials at certain frequencies if the sample lengths, L and $\alpha_1 L$, are related so that both materials resonate at a certain frequency simultaneously. Also with this technique two-sample length measurements are required, and this increases the uncertainty.

2.3 Measurement Results

The measurement consists of inserting a well-machined sample into a coaxial line or waveguide and measuring the scattering parameters. For waveguide measurements it is important to have a section of waveguide of length about two free space wavelengths between the coax-to waveguide adapter and the sample holder. This acts as a mode filter for filtering out higher evanescent modes. There are many roots to the equations for the permeability and permittivity and caution must be exercised when selecting out the correct root. At lower frequencies (< 1 GHz) the roots are usually more widely spaced and therefore root selection is simplified. Another approach to root selection is the measurement of two samples of differing lengths where the results compared to determine the correct root.

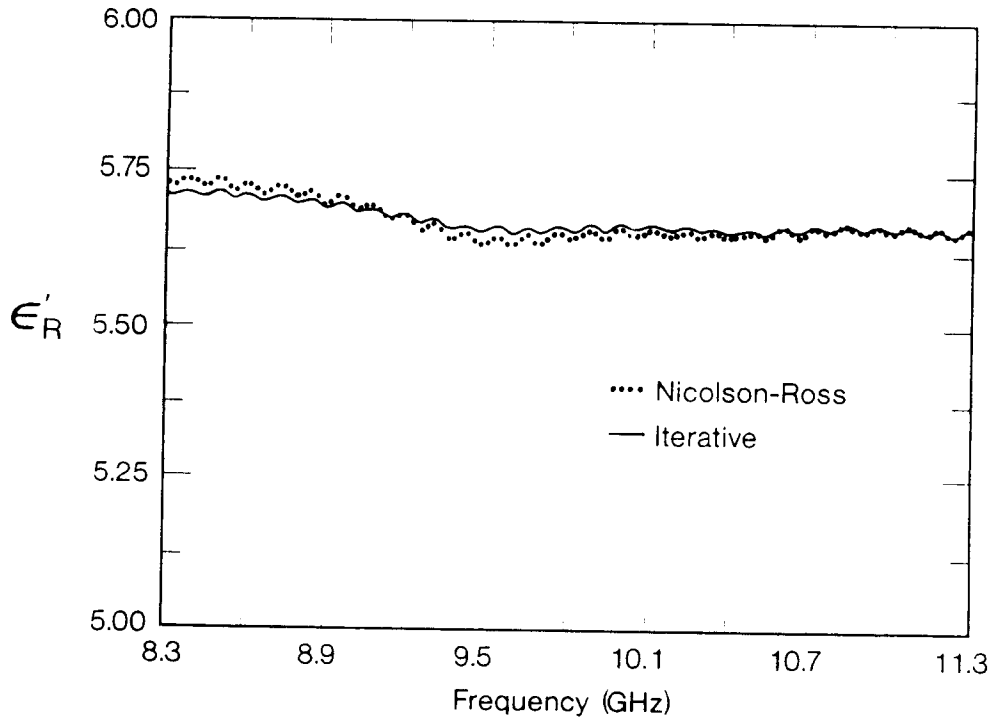

Figure 2.3: ϵ'_R of a loaded polymer in a X-band waveguide with the full S-parameter iterative technique.

2.3.1 Measurements without Gap Corrections

Various measurements have been made in waveguide and coaxial line. Some of the results of these measurements are reported in figures 2.3 through 2.14 for the full S-parameter technique and in figures 2.15 and 2.16 for the two-sample length method. The measurements reported in this section are not corrected for gaps around the sample. The effect of the air gaps is to measure values of the material parameters that are lower than the actual values. In the next section we will discuss ways of mitigating the effects of air gaps.

2.3.2 Effects of Gaps between Sample and Waveguide

Gaps between the sample holder and sample either may be corrected with the formulas given in the appendix or a conducting paste can be applied to the external surfaces of the sample that are in contact with the sample holder before insertion into the sample holder. In figure 2.17 we show a measurement of a nickel-zinc ferrite with and without a gap-filling grease. The dielectric loss factor is increased slightly by the gap filling. We suspect that part of this increase is due to the finite conductivity of the conducting grease.

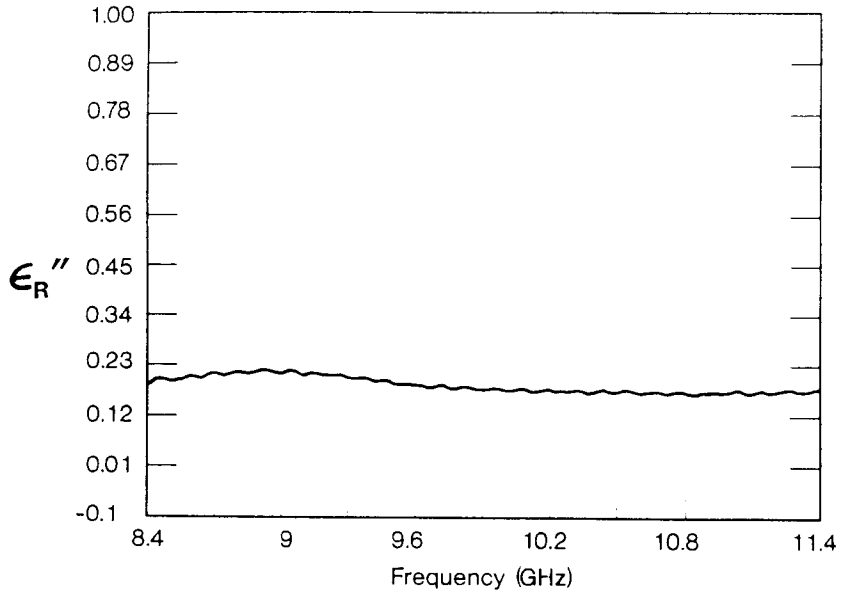

Figure 2.4: ϵ_R'' of a loaded polymer in a X- band waveguide with the full S-parameter iterative technique.

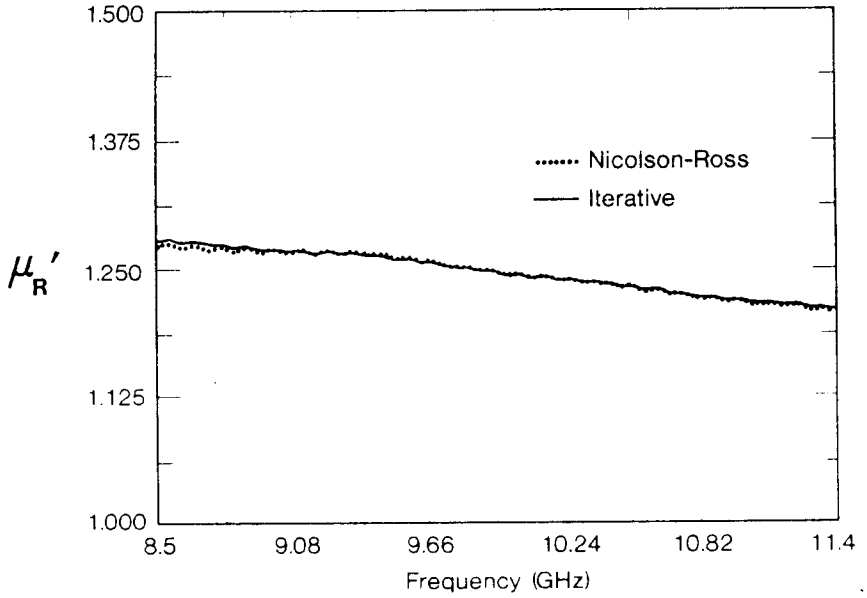

Figure 2.5: μ_R' of a loaded polymer in a X-band waveguide with the full S-parameter iterative technique.

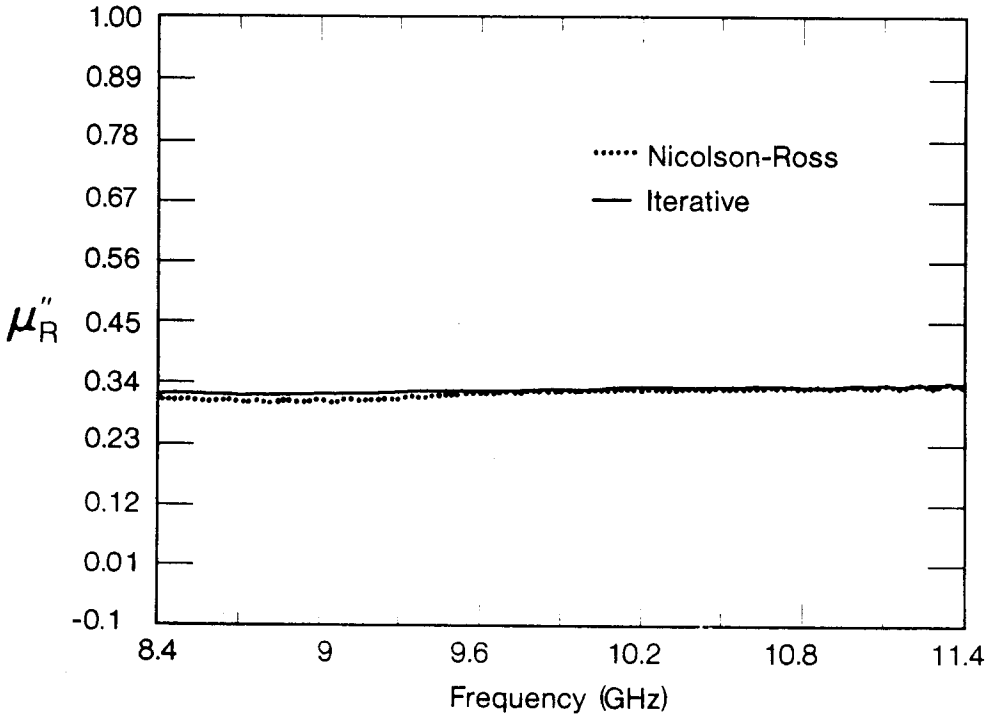

Figure 2.6: μ''_R of a loaded polymer in a X-band waveguide with the full S-parameter iterative technique.

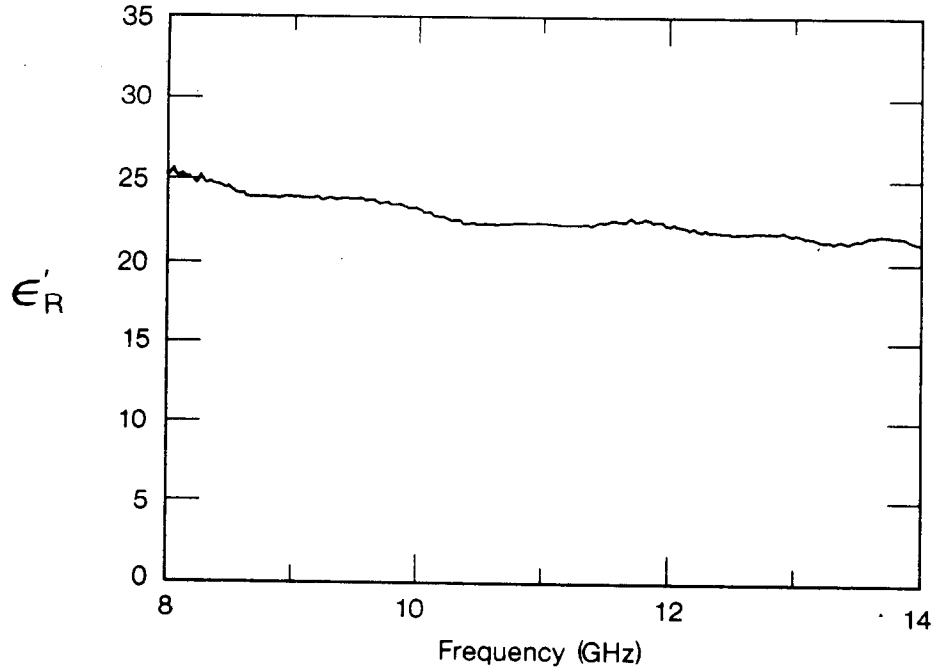

Figure 2.7: ϵ'_R of a ferrite in a X-band waveguide with the full S-parameter iterative technique.

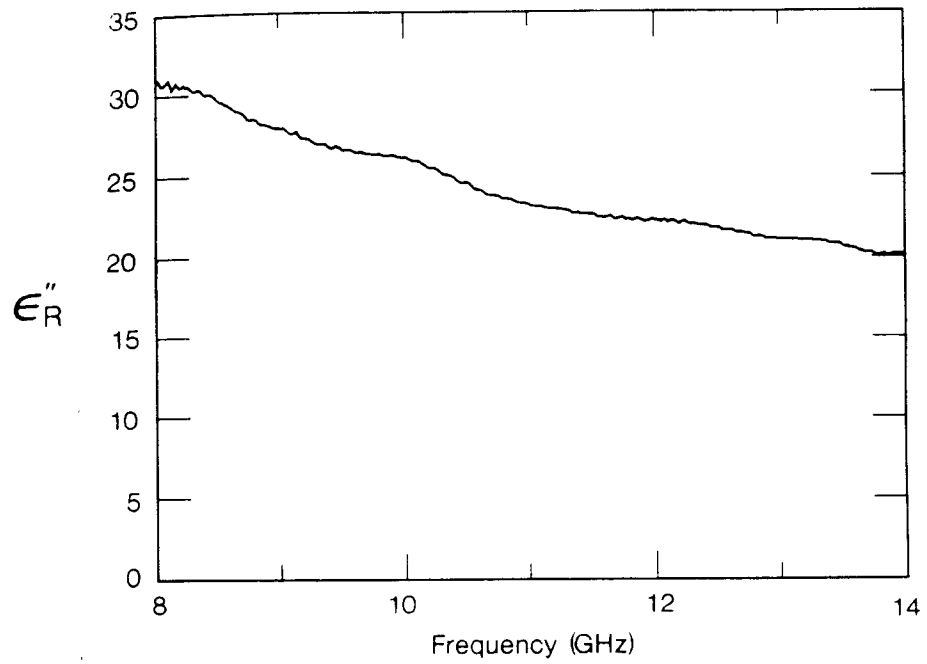

Figure 2.8: ϵ''_R of a ferrite in a X-band waveguide with the full S-parameter iterative technique.

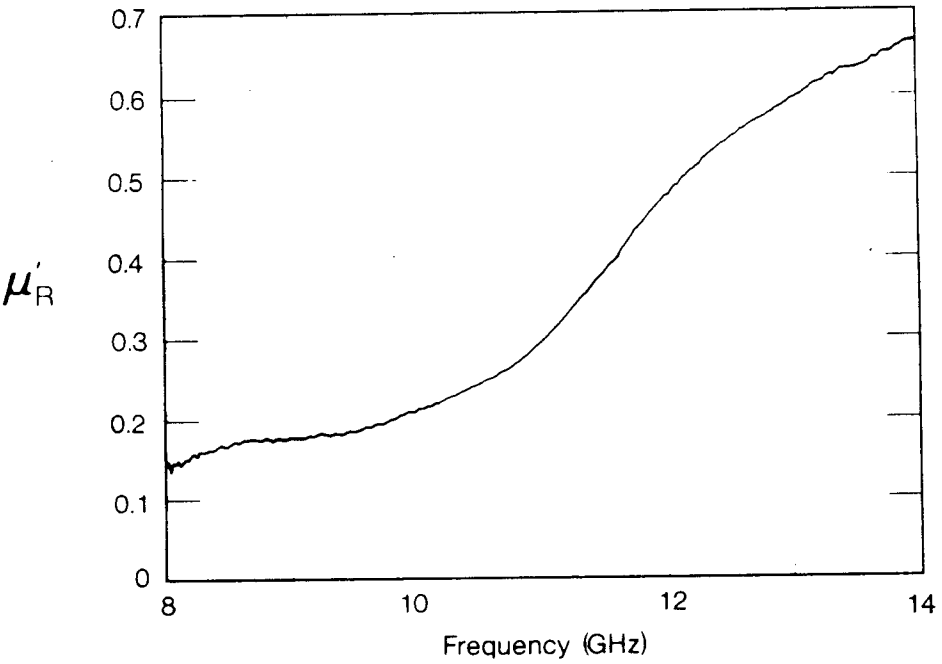

Figure 2.9: μ'_R of a ferrite in a X-band waveguide with the full S-parameter iterative technique.

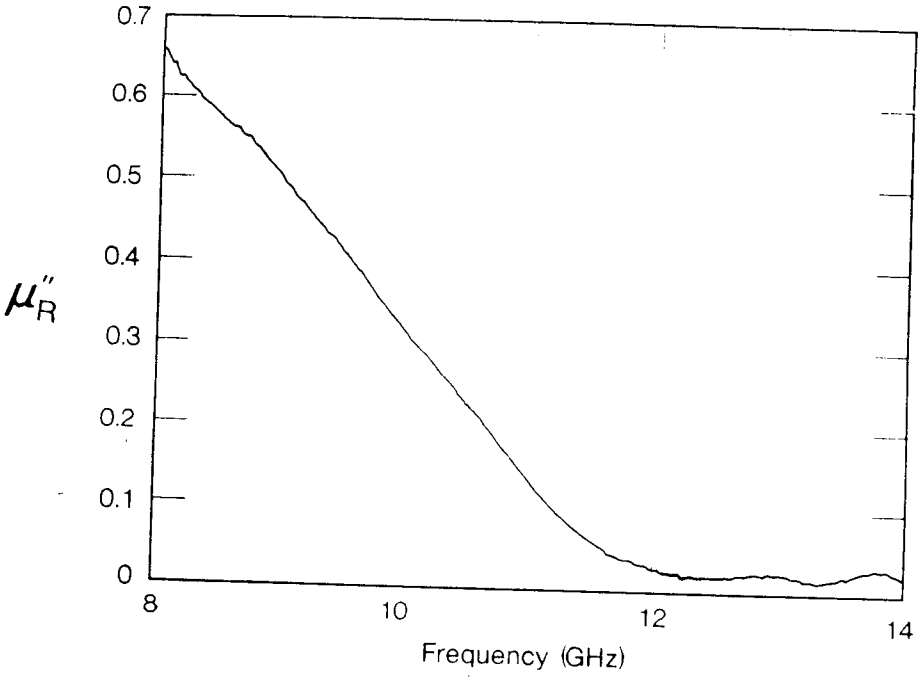

Figure 2.10: μ_R'' of a ferrite in a X-band waveguide with the full S-parameter iterative technique.

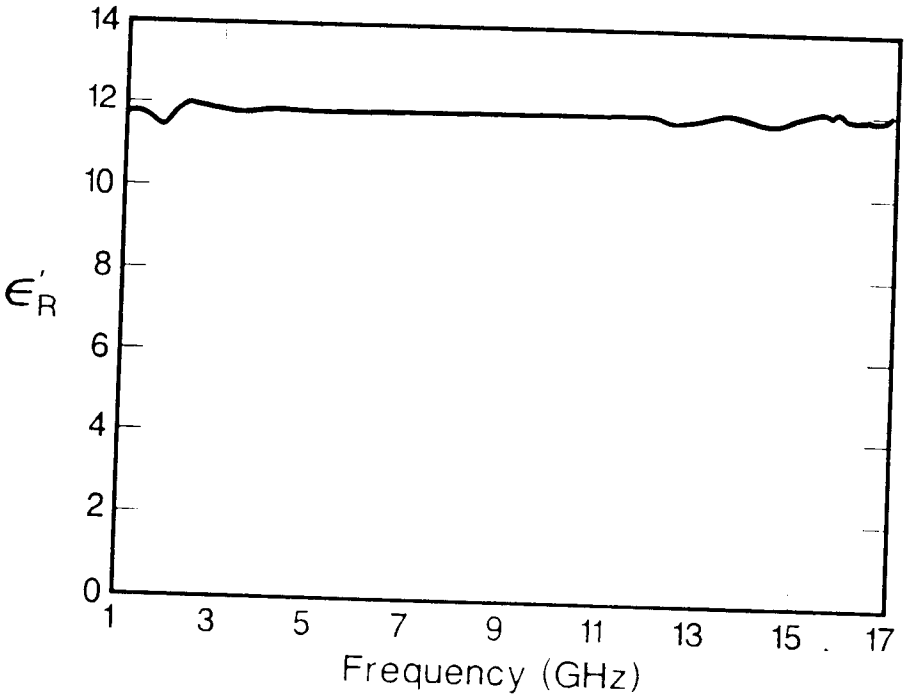

Figure 2.11: ϵ_R' of a loaded polymer in coaxial line with the full S-parameter iterative technique.

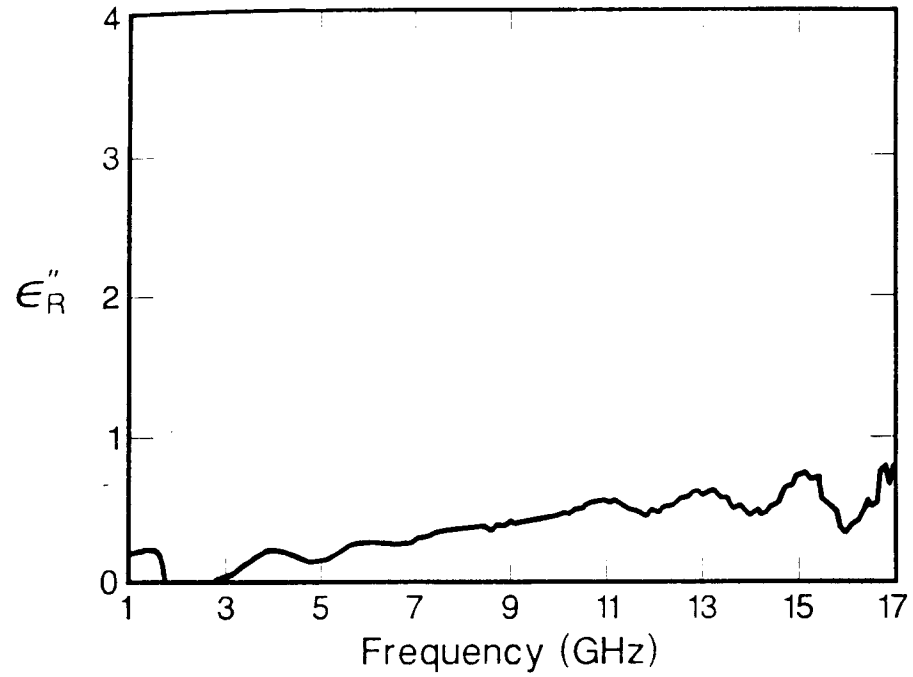

Figure 2.12: ϵ''_R of a loaded polymer in coaxial line the full S-parameter iterative technique.

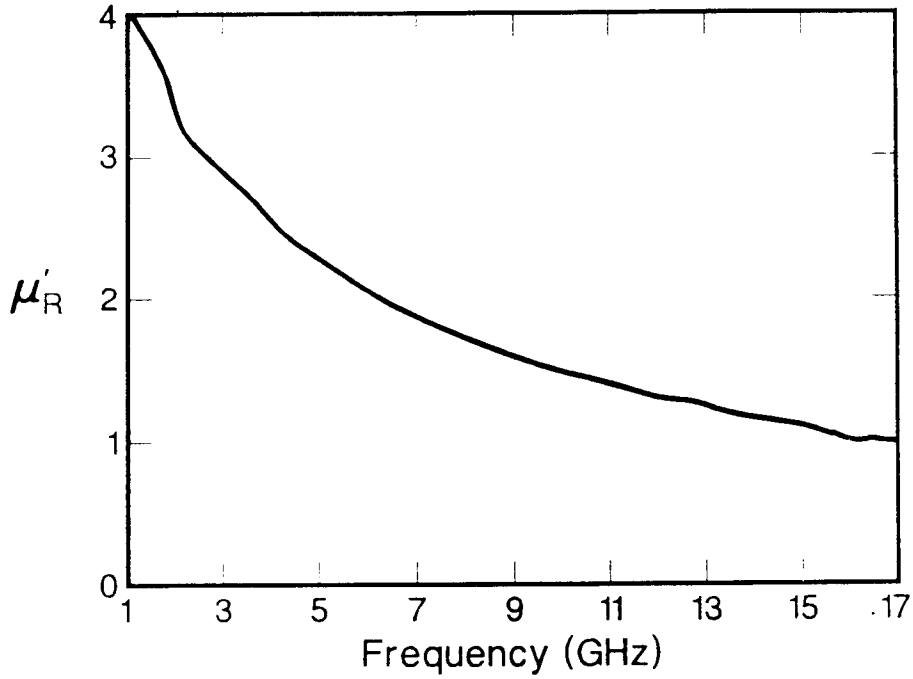

Figure 2.13: μ'_R of a loaded polymer in coaxial line with the full S-parameter iterative technique.

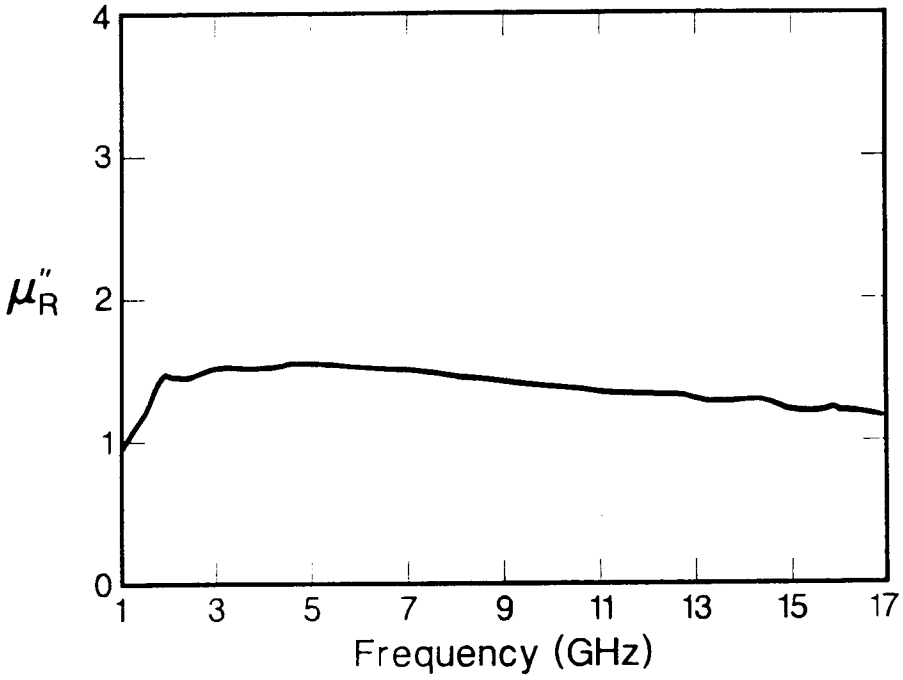

Figure 2.14: μ''_R of a loaded polymer in coaxial line with the full S-parameter iterative technique.

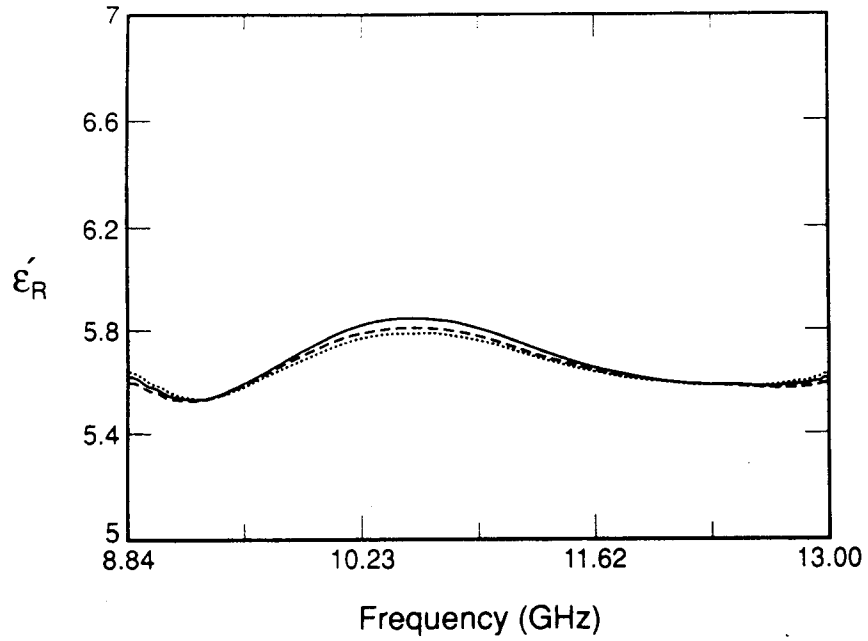

Figure 2.15: ϵ'_R of a loaded polymer in a X-band waveguide with TR method for two sample technique, for three different samples.

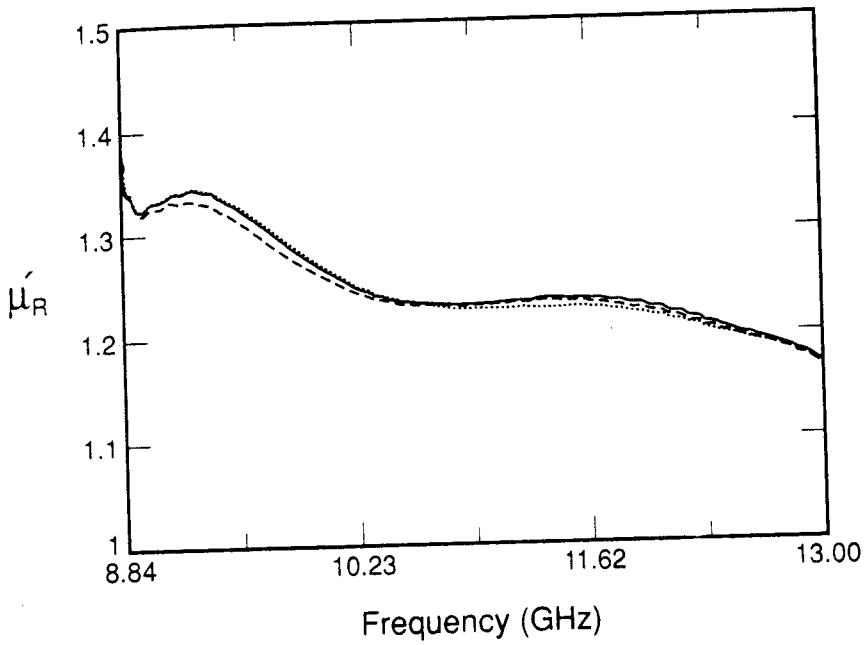

Figure 2.16: μ'_R of a loaded polymer in a X-band waveguide with TR method for two sample technique, for three different samples.

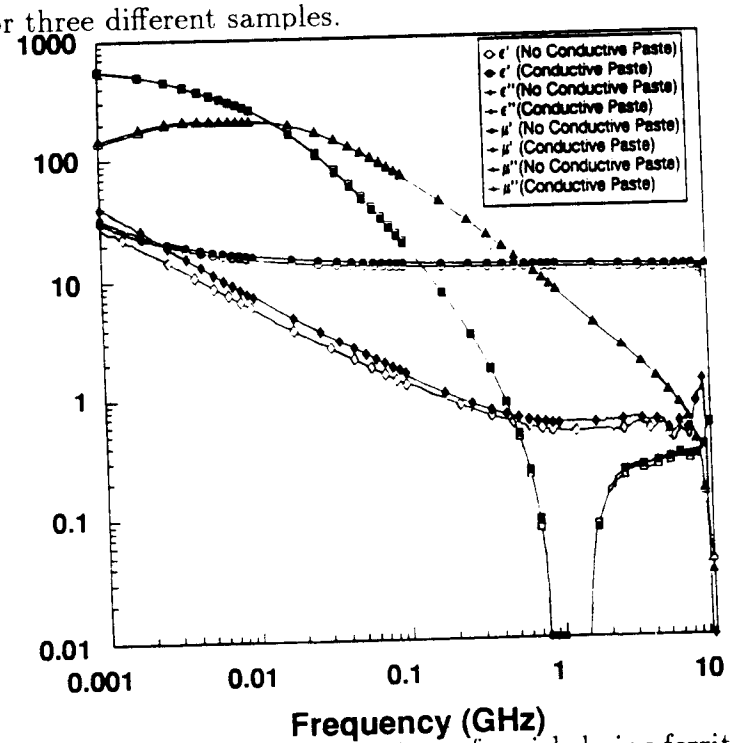

Figure 2.17: The dielectric and magnetic parameters of a nickel-zinc ferrite in a coaxial line from 1 MHz to 10 GHz with the full S-parameter iterative technique.

2.4 Permeameter

In the past permeameters have been used for high permeability materials. Rasmussen [29], Hoer [30], Powell [31], and Goldfarb [32] have all described various permeameter setups. In this section we wish to review the theory behind the permeameter.

If a toroidal sample is inserted into an azimuthal magnetic field region, the inductance is changed. If the inductance of the empty sample holder is compared to the inductance of the filled holder then it is possible to extract the complex permeability of the material.

Consider a toroid of inner diameter a and outer diameter b and height h. The material contributes an inductance of [32]

$$L_m = \frac{\mu' h \ln(b/a)}{2\pi} , \tag{2.62}$$

and the inductance of the air space is

$$L_a = \frac{\mu_0 h \ln(b/a)}{2\pi} . \tag{2.63}$$

The net change in the sample inductance when the sample is inserted into the holder is

$$\Delta L = L_m - L_a , \tag{2.64}$$

and therefore

$$\mu'_R = 1 + \frac{2\pi \Delta L}{\mu_0 h \ln(b/a)} . \tag{2.65}$$

The magnetic loss may be obtained from consideration of the core loss ΔR or resistance

$$\mu''_R = \frac{\Delta R}{\mu_0 f h \ln(b/a)} . \tag{2.66}$$

These equations are a special case of the scattering equations for short-circuit line (see eq (4.7)) in the limit as $\omega \to 0$ and through use of relation $H_\phi = E_\rho / Z$.